Sensors and Materials, Vol. 11, No. 6 (1999) 383–392
MYU Tokyo

S & M 0381

Fabrication and Study of a Shallow-Gap Pirani Vacuum Sensor with a Linearly Measurable Atmospheric Pressure Range

Bruce C. S. Chou, Chung-Nan Chen[1] and Jin-Shown Shie[1]

Precision Instrument Development Center (PIDC), 20 R&D Road VI,
Hsinchu Science-Based Industrial Park, Hsinchu 300, Taiwan, ROC
[1]Institute of Electro-Optical Engineering, National Chiao Tung University,
1001 Ta Hsueh Road, Hsinchu 300, Taiwan, ROC

(Received August 10, 1999; accepted August 10, 1999)

Key words: Pirani vacuum sensor, sacrificial layer, TMAH, freeze-drying, packaging

A Pirani vacuum sensor with a shallow gap between its heated element and its surrounding substrate heat-sink was fabricated using polysilicon as a sacrificial layer. The polysilicon was post-etched by TMAH solution, and an anti-stiction method was used in several steps of the process including a crucial freeze-drying one. The smallest spacing in this device is 0.3 μm, and via this narrow gap, the heat conductance from the gas-molecule-collisions from the hot element to the heat sink is greatly enhanced in the atmospheric pressure regime. Therefore, this Pirani vacuum sensor is capable of detecting gas pressure linearly up to around 7 bars. As for the low-pressure regime, a partial dummy compensation method reduces the ambient temperature drift effectively and pressure lower than 10^{-3} Torr was measurable. Moreover, device packaging was also studied to protect the tiny sensor from any contamination including dust and particles.

1. Introduction

Ever since the invention of the Pirani sensor in 1906,[1] the sensor has become a common unit used in nearly all vacuum equipment. Its operation is based on the pressure dependence of the heat transfer from a suspended hot resistor through a gas to its ambient. A typical Pirani gauge is used for pressure measurements ranging from 10^{-3} to 100 mbar. The precision of the detection is very poor at the extremes of this range because heat transfer through the gas becomes meaningless. Some rather complicated gauges, using either the convection or movement of gas,[2] have been constructed to extend the range of measured pressures up to 1 bar.

In the past decade, a Pirani sensor fabricated by the micromachining technique has been developed and shows very promising results to extend high and low pressure measurements.[3–10] For low-pressure measurement, Shie *et al.* proposed a sensitive device combining an effective scheme to reduce ambient temperature drift to obtain a detectable pressure as low as 10^{-7} Torr.[7] For high-pressure measurement, shallow gap formation between the hot resistor of the sensor and its heat-sink in the substrate was accomplished using sacrificial layer etching to improve its detection capability more than 1 bar.[8–10]

In this paper, we propose a Pirani vacuum sensor with a shallow gap between its heated membrane and its surrounding heat-sink. This device is capable of detecting gas pressure linearly up to around 7 bars. The detailed process is described and related characteristics of this sensor are reported.

2. Device Physics

A schematic represenstation of heat transfer through a gas between a hot plate and its surrounding heat-sink is depicted in Fig.1, where d is the spacing between the source and the sink. In this figure, the area of the hot plate is denoted as A_s, and the temperature T_s. The heat-sink has an ambient temperature of T_a. In a vacuum, the movement of these gas molecules can be treated as ideal gas behavior, with elastic collisions occurring among gas molecules. The mean free path λ of the gas can be denoted as

$$\lambda = \frac{kT}{\sqrt{2}\pi\sigma^2 P}. \tag{1}$$

Here k is the Boltzmann constant, T is the gas temperature, σ is the diameter of the gas molecule, and P is the gas pressure. For air at 27°C, the mean free path in micrometers (μm) is given by $\lambda=50/P$, with P expressed in Torr.

When thermal conductivity takes place in this configuration, the gas transports heat from the heat source to the sink. The extent of this effect increases with increasing pressure, as the amount of heat that can be conducted by the gas in the gap is proportional to the number of gas molecules. However, when the mean free path between collisions in the gas becomes smaller than the gap size d, the thermal conductance of the gas layer is no

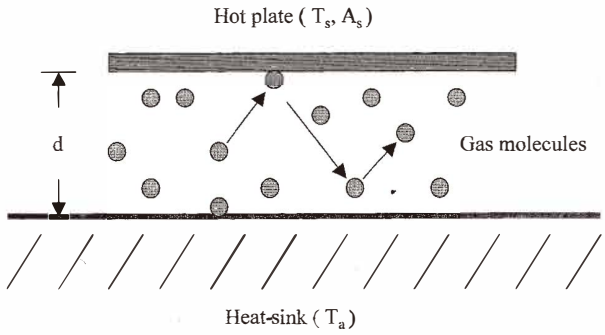

Fig. 1. Schematic representation of heat transfer by gas molecules from a hot plate to its surrounding heat-sink. The spacing between these two parallel plates is *d*.

longer proportional to pressure. This results in a stabilization of the thermal conductance of the gas. Smoluchowski showed that the thermal conductance G_g of a gas between two parallel plates as shown in Fig. 1 can be approximated by[11]

$$G_g = A_s \kappa P \left(\frac{P_t}{P + P_t}\right) \tag{2}$$

$$\kappa = \frac{\varphi}{2 - \varphi} G_a$$

$$G_a = \Lambda_0 \left(\frac{273.2}{T_a}\right)^{1/2},$$

where φ is the accommodation coefficient of the gas; G_a and Λ_0 are the free molecular conductivities at ambient temperature and 0°C, respectively; P is the gas pressure, and P_t denotes the transition pressure.

In general, there are three distinct heat-transfer regimes depending on pressure.

In the molecular-flow regime, i.e., at low pressure, the molecules move with few mutual collisions within the gap between the source and sink. In this case, P is much smaller than the transition pressure P_t, and the mean free path λ is much larger than the spacing d. From eq. (2), G_g is approximated as

$$G_g = A_s k P, \tag{3}$$

in which gas conductance is directly proportional to the gas pressure. This is the main sensing mechanism of a Pirani sensor.

In the viscous-flow regime, i.e., at high pressure, the mean free path of a gas decreases with increasing pressure. When the mean free path between collisions in the gas becomes

much smaller than the gap size d, the thermal conductivity of the gas layer is independent of pressure. Therefore, gas conductance is independent of gas pressure, and P is much larger than P_t. Equation (2) is approximated by

$$G_g = A_s k P_t. \tag{4}$$

In the transition-flow regime, the gas behavior changes from molecular flow to a viscous flow state. In this region, P is close to P_t , and the mean free path λ is approximately equal to the gap size d. The gas conductance retains the form in eq. (2), in which gas pressure is detectable but is not linearly dependent on gas conductance. Physically, P_t is defined as the value of pressure when λ is equal to d. From eq. (1), the transition pressure P_t is inversely proportional to the spacing d. Nominally, P_t is the upper limit of linearly measurable pressure for a Pirani sensor. For this reason, a narrow gap d between the heat source and sink is very desirable to boost the high pressure measurement by a Pirani sensor.

Figure 2 illustrates the typical thermal conductance of a Pirani device to its surroundings as a function of gas pressure. The total conductance G behaves as a characteristic S

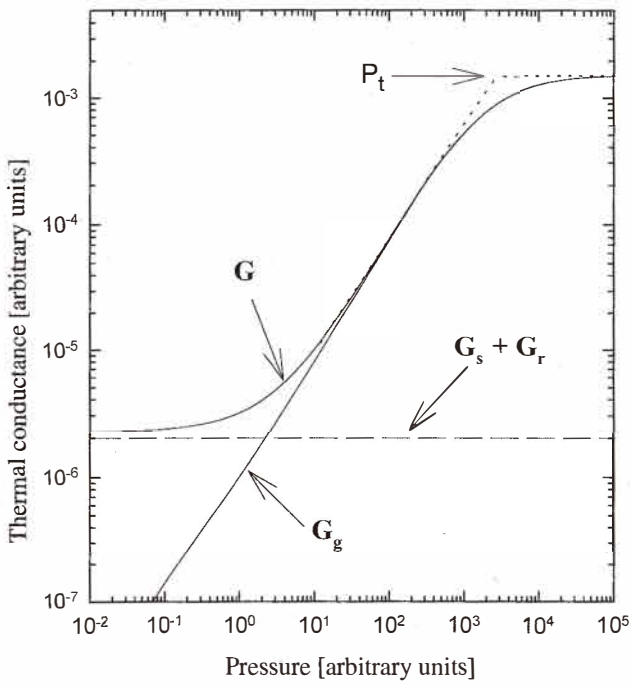

Fig. 2. Dependence of total thermal conductance and gas conductance of a typical Pirani sensor on gas pressure. A characteristic S curve represents the realistic measurement that saturates at both pressure extremes.

curve, which approaches constant values at both ends. Below the turning point where the transition pressure is defined, the gas conductance G_g becomes linearly dependent on the pressure variation, as does the total conductance G. Below this point, the gas behavior belongs to the molecular flow state, while at high vacuum, the total conductance G approaches a minimum value G_0 that is the sum of solid and radiative conductance. Therefore, to function as a high-vacuum sensor, it is necessary to reduce the residual conductance G_0 by proper design of the device and to modify the calibration as analyzed in our previous report.[10]

3. Sensor Fabrication

Floating microstructures with shallow gaps underneath can be made by surface micromachining techniques using various approaches.[8–9,12] In our device, polysilicon is used as a sacrificial layer to form small spacings. Figure 3 shows the SEM of a fabricated device, where an active floating membrane with an area of 50×50 μm^2 and an on-substrate dummy resistor for temperature compensation[6–7] are fabricated simultaneously on the same chip. Each kink-shaped lead is 80 μm long and 10 μm wide. The sensor has a resistance of 200 Ω and a temperature coefficient of resistance (TCR) of 0.28 %/°C.

The process flow of the corresponding device in Fig. 3 is schematically shown in Fig. 4. First, a 0.3-μm-thick polysilicon layer was deposited on an oxidized silicon wafer and patterned as the sacrificial layer. An additional but important step is to etch part of the sacrificial polysilicon to the desired depth of 0.15 μmm. This forms the bushing patterns in the sacrificial layer that act as molds for the following Si-rich nitride, where the bushings become part of the Si-rich nitride. The floating membrane was made of 0.4-μm-thick low-stress silicon-rich nitride deposited by LPCVD on the polysilicon.[13] A 0.1-μm-thick

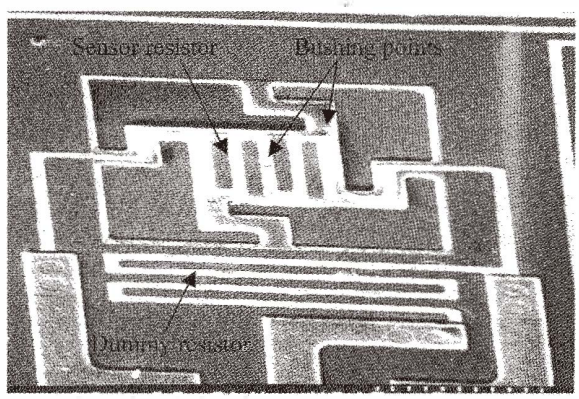

Fig. 3. SEM of the device fabricated by the polysilicon sacrificial layer technique.

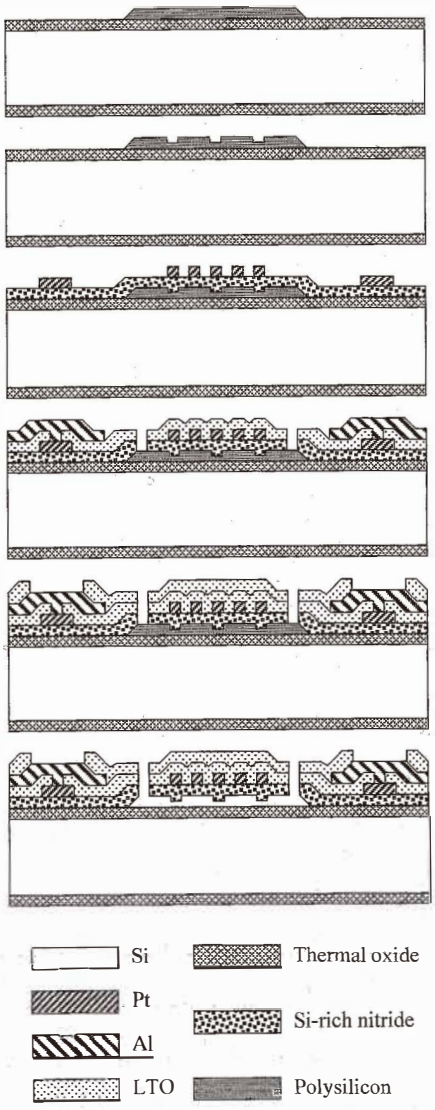

Fig. 4. Brief process flow of the Pirani sensor shown in Fig. 3.

platinum film was deposited on the nitride by e-gun evaporation for both the sensor and the dummy. A 0.8-μm-thick layer of low-temperature oxide (LTO) was deposited for the purpose of metal passivation. The structures were released in a TMAH solution at 80°C and rinsed in sequence in water, water and ethanol (or isopropyl alcohol) solution, and pure ethanol. Finally, using the t-butyl alcohol freeze-drying method,[14] we obtained the floating sensor structures.

4. Anti-Stiction

Stiction is a notorious cause of malfunction in microdevices. Surface micromachined structures which have been fabricated using the wet sacrificial layer etching technique can be pulled down to the substrate by capillary forces during drying. It was reported that this problem could be solved by the t-butyl alcohol freeze-drying method.[14] The t-butyl alcohol is a solid at room temperature (the freezing point is about 25°C); therefore, it is possible to carry out freeze-drying without special cooling equipment. This method only requires a hot plate, a normal refrigerator and a simple vacuum system. Modified conditions of freeze-drying for the Pirani sensor are as follows. After TMAH etching, wafers were put into DI water to rinse off residual TMAH residues. Then, we transferred the wafers to a 50%water-50%ethanol (or isopropyl alcohol) solution by volume. Finally, the wafers with microstructures were dehydrated with pure ethanol (or isopropyl alcohol). After dehydration, the wafers were immersed in t-butyl alcohol. When room temperature is below the melting point of the alcohol, the alcohol can be liquidized by warming on a hot plate. Next, the wafers in t-butyl alcohol were placed in a refrigerator. The alcohol was frozen in a few minutes. Eventually, the wafers were transferred to a vacuum system evacuated by a mechanical pump. The frozen t-butyl alcohol sublimated and dried wafers were obtained. Using this freeze-drying method combined with the bushing structures, a Pirani sensor with a 0.3 μm shallow gap was fabricated without the problem of stiction. A flow chart illustrating this anti-stiction method is shown in Fig. 5.

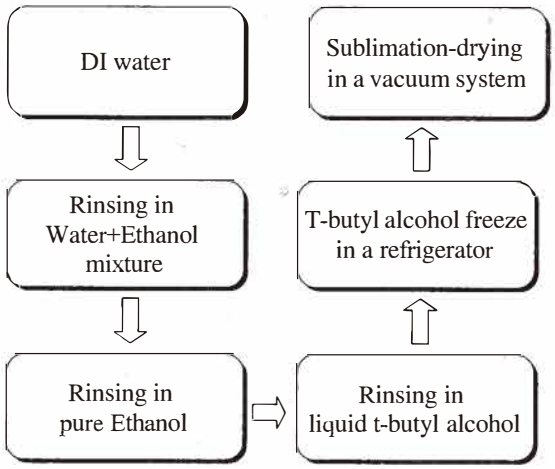

Fig. 5. Flow chart of the freeze-drying method for device fabrication.

5. Results and Discussion

Surface contamination and particles covering the sensor body alter the gauge calibration by changing the thermal behaviour of the sensor itself in terms of surface emissivity, solid conductivity and the accommodation coefficient of the incident gas molecules. Sensor packaging, therefore, should be carefully managed to avoid contamination. A commercially available TO-5 metal can was adopted as a chip-form package for our sensor. Two forms of packaging are proposed here. One has a cap soldered with metal mesh, and another has a cap with laser-drilled microholes. These packed sensor modules are shown in Fig. 6.

The sensor module was then installed in a vacuum system for calibrating pressures ranging from 10^{-6} Torr to 1 atm. A nitrogen gas source was linked through a needle valve to the chamber for the adjustments of pressure that was monitored by a set of MKS Baratron vacuum gauges to cover the entire pressure range. Another nitrogen-filled high-pressure system (Budenberg 450C) was used for calibrations ranging from 0.7 to 150 atm.

A constant-bias bridge circuit was adopted for signal measurement. The partial compensation method that had been developed in our previous work[7,10] was used to eliminate the ambient temperature drift. The estimated membrane temperature in our experiment was about 50°C at high pressure. The signal voltage was measured by a digital

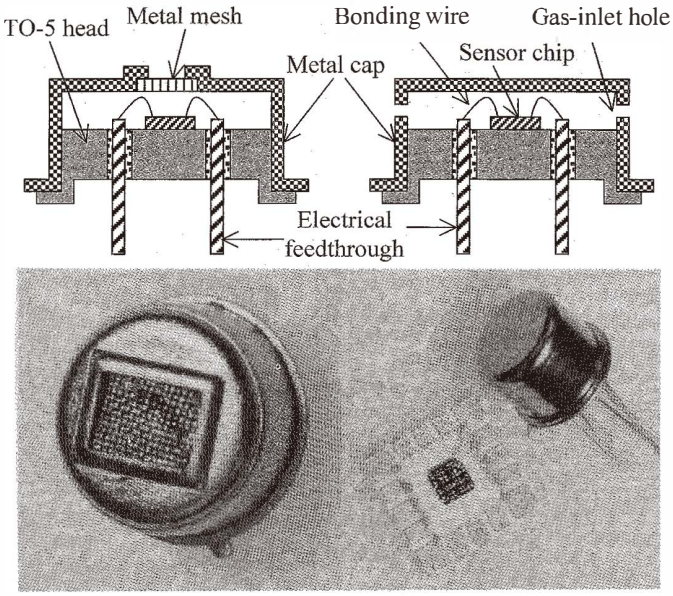

Fig. 6. Chip-form packaging using a TO-5 metal head for the micro-Pirani sensor to prevent contamination.

voltmeter (DVM), which was sampled and recorded by a PC through a IFEE 488 GPIB interface connected to the voltmeter.

Figure 7 shows the curve of the output voltage as a function of the absolute pressure of the gas. The curve has a characteristic S shape similar to the total thermal conductance curve shown in Fig. 2. At low pressures, the heat loss through the gas is negligible compared to the loss through the solid and by radiative mechanisms; hence, the output voltage is essentially constant. At very high pressures, the thermal conductivity of the gas becomes independent of pressure when the voltage reaches a maximum. The useful range for pressure sensing occurs between these extremes. It is noted that in this device the linearly detectable high pressure is as high as 7 bars. This excellent capability for high-pressure measurement is obviously enhanced by the shallow gap formed between the heat source and sink. This same observation has been made by others.[8] From the traditional theory of gas kinetics, eq. (1) is used to predict the physical transition pressure of a Pirani sensor. For this device, the calculated P_t should be about 200 Torr. Therefore, it implies an enhancement factor for the transition pressure when the gap approaches microscopic dimensions, where the statistical theory of gas kinetics in macroscopic space should be modified. For this device, the enhancement factor is about 27.

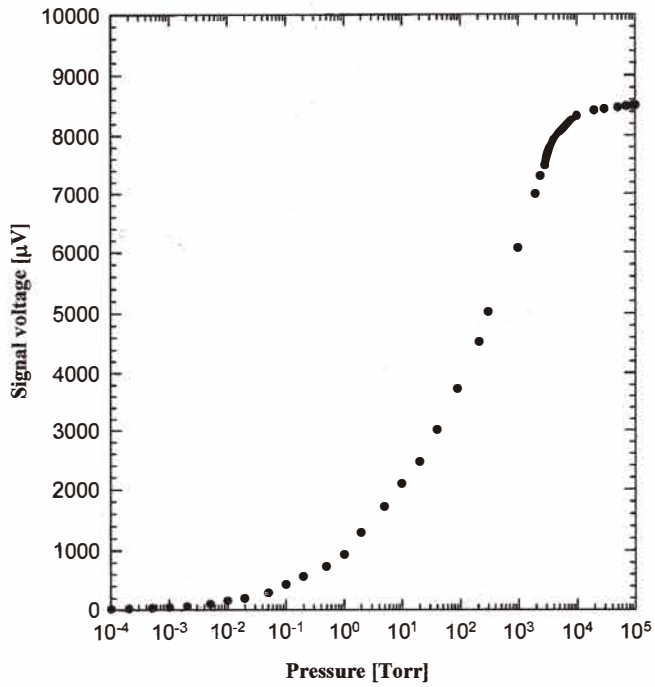

Fig. 7. The measured signal of the shallow-gap sensor as a function of pressure with the constant bias circuit. Very high pressure detection linear up to 7 bars is demonstrated.

6. Conclusion

A shallow-gap Pirani vacuum sensor was fabricated using polysilicon sacrificial layer etching. Bushing structures combined with a freeze-drying method were adopted to resolve the stiction problem due to capillary forces during the drying of the microstructures. Linear pressure measurements as high as 7 bars were carried out using this device. Hence, the micro-Pirani sensor can be used not only as a vacuum sensor but also as a pneumatic pressure transducer, which has different detection physics from that of capacitive and piezoresistive pressure sensors. Comparatively, this device is advantageous due to smaller dimensions and a wider dynamic range and it also has a simpler structure. It is expected that by using a shallow-gap device with a large area and a more sensitive readout circuit, better performance both at high and low pressure can be obtained.

Acknowledgements

The authors express their appreciation to the Semiconductor Research Center of NCTU and the Nano Device Laboratory of NSC for the sample preparation and device fabrication.

References

1 M. Pirani: Verh. Dtsch. Phys. Ges. **8** (1906) 686.
2 P. E. Seiden: Rev. Sci. Instrum. **28** (1957) 657.
3 A. W. Van Herwaarden and P. M. Sarro: Sensors and Actuators **8** (1985) 187.
4 C. H. Mastrangelo and R. S. Muller: IEEE J. Solid-State Circuits **26** (1991) 1998.
5 A. M. Robinson, P. Haswell, R. P. Lawson and M. Parameswaran: Rev. Sci. Instrum. **63** (1992) 2026.
6 P. K. Weng and J. S. Shie: Rev. Sci. Instrum. **65** (1994) 492.
7 J. S. Shie, B. C. S. Chou, and Y. M. Chen: J. Vac. Sci. Technol. A **13** (1995) 2972.
8 H. Baltes and O. Paul: Sensors and Materials **8** (1996) 409.
9 B. C. S. Chou and J. S. Shie: Transduces'97 Technical Digest 1997 (Chicago, 1997) 1465.
10 B. C. S. Chou: Ph. D. dissertation (1997) NCTU, Taiwan, ROC.
11 M. Von Smoluchowski: Ann. Physik **35** (1911) 983.
12 R. T. Howe: J. Vac. Sci. Technol. B **6** (1988) 1809.
13 B. C. S. Chou, J. S. Shie and C. N. Chen: IEEE Electron Device Lett. **18** (1997) 599.
14 T. Inoue and H. Osatake: Arch. Histol. Cytol. **51** (1988) 53.

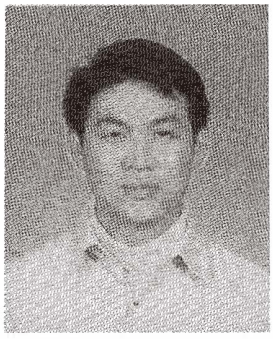

Bruce C. S. Chou received his M.S. degree from National Tsing Hua University in 1991 and Ph.D. degree from the Institute of Electro-Optical Engineering, National Chiao Tung University, Hsinchu, Taiwan, in 1997, in Si-based micromachining and microthermal sensor fabrication. Since then, he has been working at PIDC on optical MEMS and CMOS-based microsystems.